Short communication

Improvement in the low temperature performance of gelled polymer lithium-ion cells

Weibing Xing[a,*], Hiromu Sugiyama[b]

[a]Wilson Greatbatch Technologies Inc., 10,000 Wehrle Drive, Clarence, NY 14031, USA
[b]Hitachi Maxell Ltd., 1-1-88 Ushitora, Ibaraki, Osaka 567, Japan

Abstract

Improved low temperature performance of gelled polymer lithium-ion cells was achieved by optimizing both electrolyte formulations and processes of gelled polymer electrolyte preparation and electrode coating. In the electrolyte system, $LiPF_6$ in ethylene carbonate (EC)/ propylene carbonate (PC), the highest ionic conductivity value was found when the $LiPF_6$ concentration was around 1.0 M and the EC:PC ratio was around 1:1 (w/o) over a temperature range of −20 to 20 °C. Low temperature electrochemical performance showed that cells with lower EC content electrolytes delivered finite discharge capacities under group-special-mobile (GSM) conditions, compared with nearly zero discharge capacities for cells with higher EC content electrolytes. Electrochemical impedance study showed that cells with higher EC content electrolytes had much larger impedance at low temperature than cells with lower EC content electrolytes. The best low temperature electrochemical performance was obtained when electrodes were paste-coated and the gelled polymer electrolyte was cured under ultra violet radiation. Cells prepared this way were shown to have good interfacial properties both at room temperature and at −20 °C.
© 2003 Elsevier Science B.V. All rights reserved.

Keywords: Electrolyte ionic conductivity; Gelled polymer lithium-ion cells; Low temperature performance; Group-special-mobile (GSM) discharge conditions

1. Introduction

Lithium-ion cells with gelled polymer electrolytes are potential candidates as high energy density power sources. They may be used in, for example, portable electronic devices because of their light weight. One of the challenges the gelled polymer lithium-ion cells face is to deliver sufficient capacities at low temperatures and/or at high current pulses, the condition required in some electronic device applications. Lithium-ion cells with liquid electrolytes face the same challenge. To address this challenge, many research and development efforts have been devoted to new organic solvents, electrolyte systems and electrolyte additives in order to improve low temperature performance of lithium-ion cells. Examples of these efforts include syntheses of acyclic, asymmetric alkyl carbonates, especially asymmetric alkyl methyl carbonates [1], and halogenated organic solvents [2], and the use of multiple-component organic solvents [3–5], pyrocarbonate additives

[6,7] and electrolytes with different lithium salts [8]. We reported previously that, a moderate increase of usable discharge capacity at low temperature was achieved by adding pyrocarbonates to gelled polymer lithium-ion cell components [9].

In this study, we report that the low temperature performance of gelled polymer lithium-ion cells can further be improved by optimizing both electrolyte formulations and processes of gelled polymer electrolyte preparation and electrode coating.

2. Experimental

2.1. Solution ionic conductivity measurements

Various electrolytes were prepared using a 5 ml flask inside an argon filled glove box. The liquid electrolyte solutions were put in YSI conductivity cells (model 3403). The cell constant of the conductivity cells was checked with 0.1 M KCl aqueous solution. The temperature of the samples was controlled in a Tenney Environmental Test Chamber, from −20 to 20 °C. The samples were

* Corresponding author. Tel.: +1-716-7595475; fax: +1-716-7595480.
E-mail address: wxing@greatbatch.com (W. Xing).

stabilized in the chamber for at least one hour prior to maturing conductivity measurements. Solution impedance was measured with a QuadTech RLC meter at 1 kHz and 1 V ac. From the cell constant ($1.0 \, \text{cm}^{-1}$), conductivity values of the electrolytes were calculated.

2.2. Preparation of cells with paste-coated electrodes and thermally cured SPEs

The process of making gel polymer lithium-ion cells with paste-coated electrodes and thermally cured solid polymer electrolytes (SPEs) was developed at Electrochem, a division of Wilson Greatbatch Technologies Inc. [10]. The anode was made by hot-pressing a paste-like coating material consisting of graphite active material, carbon black, polyvinylidene fluoride (PVDF) binder, and a liquid electrolyte solution consisting of $LiPF_6$ in ethylene carbonate (EC)/propylene carbonate (PC) onto a copper foil. The cathode was made in a similar way with $LiCoO_2$ active material on aluminum foil. The coated electrodes were heated at $114 \pm 2 \, °C$ for 12 min. After curing, the electrodes were trimmed with scissors to the desired dimensions and the cell leads or current collectors were cleaned with a pencil brush.

Three monomers with acryloyl functionalities were used in the gel polymer electrolyte precursor. Examples were 2-ethoxyethyl acrylate, ethylene glycol ethyl carbonate methacrylate and tri(ethylene glycol) dimethacrylate. The precursor solution of the gel solid polymer electrolyte was prepared by mixing the monomers with a liquid electrolyte consisting of $LiPF_6$ and EC/PC plasticizers. Polymerization of the SPE precursor was initiated by thermal activation of benzoyl peroxide, at $79 \, °C$ for 16 min. A non-woven fabric was used for mechanical reinforcement of the SPE.

In cell assembly, the SPE was sandwiched between the electrodes and the anode/SPE/cathode stack was sealed in a foil/poly outer bag. The active cell size was $3.8 \, \text{cm} \times 6.7 \, \text{cm}$ ($25.5 \, \text{cm}^2$) and the total thickness of the cell was about 0.6 mm. The nominal cell capacity was about 50 mAh.

2.3. Preparation of cells with slurry-coated electrodes and UV cured SPEs

The process of making gel polymer lithium-ion cells with slurry-coated electrodes and UV cured SPEs was developed at Hitachi Maxell Ltd. [11]. The anode slurry consisted of a natural graphite active material, a conductive carbon, PVDF binder, and N-methyl-2-pyrrolidinone solvent. The cathode slurry used $LiCoO_2$ as the active material which was mixed with other ingredients similar to the anode slurry. The slurries were coated on copper and aluminum foils for anodes and cathodes, respectively. After drying, the electrodes were pressed. The electrodes were die-cut to a size of $4.0 \, \text{cm} \times 6.9 \, \text{cm}$ ($27.6 \, \text{cm}^2$) for anodes and $3.8 \, \text{cm} \times 6.7 \, \text{cm}$ ($25.5 \, \text{cm}^2$) for cathodes. The die-cut electrodes were dried again in a vacuum oven at $100 \, °C$ overnight.

The precursor solution of the SPE consisted of a liquid electrolyte, $LiPF_6$ in EC/PC, and a multi-functionality monomer, dipentaerythritol penta-/hexa-acrylate.

In cell assembly, the anode and the cathode were separately placed inside polyethylene bags. A non-woven fabric (NKK, 51 μm thick), used for reinforcing the strength of the SPE, was laid on the anode. The bags were then filled with a sufficient amount of SPE precursor solution and sealed under vacuum to assist wetting of the electrodes. The wetting of the electrodes took about 1 h. Curing of the electrodes and the SPE was initiated by activation of Lucirin TPO photo initiator under UV radiation generated by a pulse UV lamp (Xenon, RC-500B). During curing, the UV radiation lasted for about 7.6 s under $315 \, \text{mJ/cm}^2$ intensity. After curing, the anode, the cathode and the SPE separator were stacked together. The anode/SPE separator/cathode stack was sealed in a foil/poly outer bag.

2.4. Preparation of cells with paste-coated electrodes and UV cured SPEs

When combining the above two methods for cell making, a non-woven fabric was first soaked with the SPE precursor solution. The wetted fabric was then laid on a thermally cured anode (paste-coated) and sealed with a polyethylene bag under vacuum. The wetted fabric was then subjected to UV radiation. After SPE curing, a thermally cured cathode (paste-coated) was laid on the SPE. The anode/SPE/cathode stack was sealed in a foil/poly outer bag.

2.5. Low temperature testing

Prior to low temperature tests, the cells were cycled between 2.75 and 4.20 V for five cycles and then fully charged at room temperature at 0.4C. The cells were then cooled to $-20 \, °C$. After being stabilized at $-20 \, °C$ for 2 h, the cells were discharged under group-special-mobile (GSM) conditions to a 3 V cutoff potential. GSM discharge conditions consisted of a series of 4C current pulses with 0.6 ms duration. The background current between the high current pulses was 0.3C with 4.0 ms duration. Discharge capacities are calculated as the ratio of the GSM discharge capacity at $-20 \, °C$ to the low rate discharge capacity at room temperature. The 1C rate corresponds to a current density of $2 \, \text{mA/cm}^2$.

3. Results and discussion

3.1. Ionic conductivity of electrolytes

Table 1 and Fig. 1 show ionic conductivities of electrolytes, $LiPF_6$ in EC:PC = 1:1 (w/o), as functions of $LiPF_6$ molarity and temperature. The results showed that 1.0 M $LiPF_6$ gave consistently slightly higher conductivity values between -20 and $10 \, °C$ compared with other concentrations. At $22 \, °C$,

Table 1
Ionic conductivities of electrolytes containing EC:PC = 1:1 (w/o) vs. $LiPF_6$ molarity and temperature

Molarity $LiPF_6$ (M)	Conductivity (mS/cm)				
	20 °C	10 °C	0 °C	−10 °C	−20 °C
0.8	6.478	4.118	2.808	1.775	1.012
1.0	6.611	4.372	3.099	2.049	1.229
1.2	6.674	4.241	2.946	1.895	1.098
1.4	5.778	3.364	2.172	1.282	0.661
1.6	5.789	3.223	2.039	1.177	0.592

Table 2
Ionic conductivities of electrolytes with 1.0 M $LiPF_6$ vs. EC/PC ratio and temperature

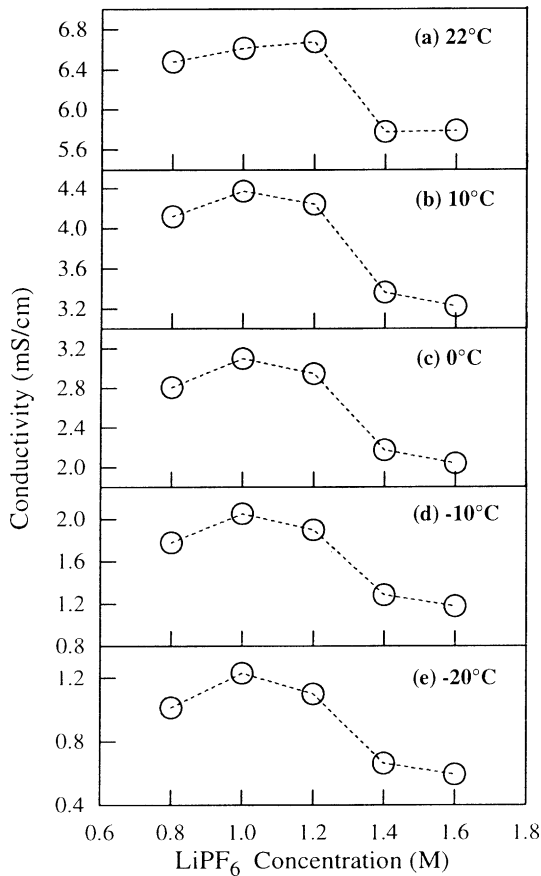| EC/PC (w/o)	Conductivity (mS/cm)				
	22 °C	10 °C	0 °C	−10 °C	−20 °C
1.4	6.093	4.254	2.978	1.915	1.127
1.2	6.354	4.357	3.014	1.886	1.065
1.0	6.106	4.26	2.934	1.91	1.113
0.8	5.559	3.876	2.715	1.722	0.994
0.6	5.294	3.664	2.555	1.632	0.963

Fig. 1. Electrolyte conductivity vs. $LiPF_6$ concentration and temperature. EC:PC = 1:1 (w/o).

Fig. 2. Electrolyte conductivity vs. EC/PC ratio and temperature. $LiPF_6$ concentration = 1.0 M.

1.2 M $LiPF_6$ gave a slightly higher conductivity value than that of 1.0 M $LiPF_6$. An appreciable decrease in conductivity was observed when $LiPF_6$ concentration was higher than 1.2 M at all temperatures.

Table 2 and Fig. 2 show ionic conductivities of electrolytes, 1.0 M $LiPF_6$ in EC/PC, as functions of EC/PC ratio and temperature. The EC/PC ratio of 1.2 (w/o) gave slightly higher conductivity values between 0 and 22 °C, compared with other EC/PC ratios. Between −10 and −20 °C, the EC/PC ratio of 1.0 gave slightly higher conductivity value than EC/PC = 1.2. An appreciable decrease in conductivity was observed when EC/PC ratio was smaller than 1.0 at all temperatures.
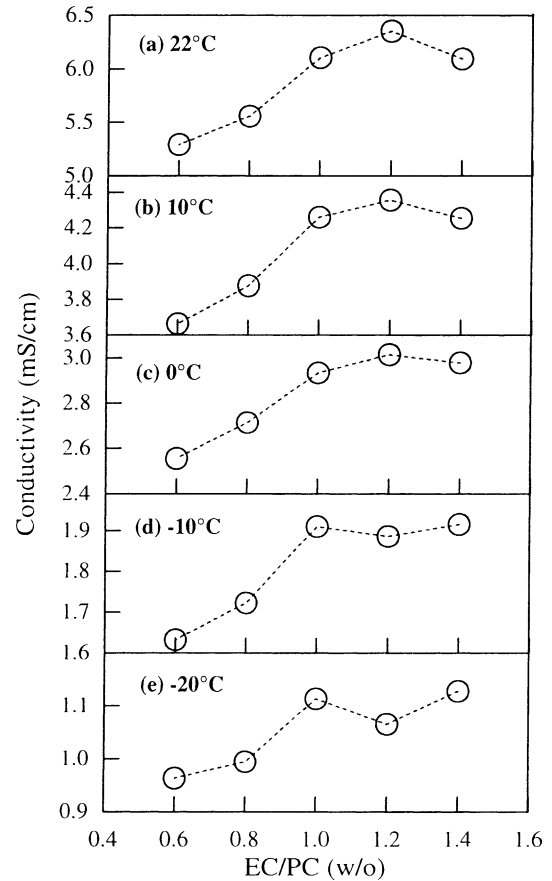
3.2. Cell performance under GSM discharge conditions at −20°C

Table 3 summarizes the room and low temperature performance of cells prepared by different methods and with different EC/PC ratios. The data in Table 3 represent the average performance in each cell series. The cells were grouped according to the preparation methods and electrolytes used, as indicated in Table 3. Each cell series contained at least two cells except for those whose low temperature GSM discharge capacities were nearly zero, e.g. series A1, A2 and B1. In cell series C2 where optimal low temperature performance was shown, more than twenty cells were

Table 3
Room and low temperature performances of cells prepared by different methods and with different EC/PC ratios

Cell series	Electrode coating method	EC:PC (w/o)	SPE curing method	Capacity at 0.2C (mAh)	C rate (% vs. 0.2C)		GSM capacity at −20 °C (% vs. RT)
					1C	2C	
A1	Slurry	1.1:1	UV	56.5	87	37	0
A2	Slurry	1:1[a]	UV	54.3	–	–	0
B1	Paste	2:1	Thermal	51.3	95	57	0
B2	Paste	1.1:1	Thermal	46.5	97	91	2.7
B3	Paste	1:1	Thermal	54.2	95	50	6.1
B4	Paste	1:1	Thermal[b]	46.0	95	53	4.5
B5	Paste	1:1	Thermal[c]	50.0	97	78	4.3
C1	Paste	2:1	UV	56.9	97	92	0
C2	Paste	1:1	UV	51.6	96	91	7.8

The molar concentration of $LiPF_6$ in electrolytes was 1.0 M, or otherwise indicated.

[a] With 1.22 M $LiPF_6$.
[b] 40 °C for 65 h.
[c] 60 °C for 3.5 h.

prepared to confirm the results. The molar concentration of $LiPF_6$ in electrolytes was 1.0 M in all cells, or as otherwise indicated.

In the cell series A1 and A2, slurry-coated electrodes, UV cured SPEs and electrolytes with slightly different EC/PC ratios were used. The $LiPF_6$ concentration in series A2 was 1.2 M. The two series of cells could normally be discharged at room temperature. However, they showed no discharge capacity when they were cooled to −20 °C and under GSM discharge conditions.

In cell series B1 to B5, paste-coated electrodes, thermally cured SPEs and electrolytes with various EC/PC ratios were used. $LiPF_6$ concentration was 1.0 M in the electrolytes. The B-series showed improved C rate performance at room temperature, compared with that of the A-series. When the cells were cooled to −20 °C and under GSM discharge conditions, cells with 2:1 EC/PC ratio delivered no capacity. Cells with 1.1:1 and 1:1 EC/PC ratios (cell series B2 and B3) gave average 2.7 and 6.1% discharge capacities, respectively, versus those at room temperature. Figs. 3(a) and (b) compare typical GSM discharge profiles at −20 °C for cell series B2 and B3. The triangles and the circles in the figure represent potential profiles of high current pulses and low current background, respectively. The longer high current pulse discharge time for series B3 clearly indicates an improved low temperature performance, compared with series B2.

In cell series B4 and B5, SPEs were cured at lower temperatures and for longer times, 40 °C for 65 h and 60 °C for 3.5 h, respectively, compared with 79 °C and 16 min used for cell series B1–B3. Cells with these SPEs had comparable room temperature performance with other B-series. However, the low temperature performance of series B4 and B5 was not further improved. The average GSM discharge capacities at −20 °C for series B4 and B5 were 4.3 and 4.5% versus those at room temperature, respectively.

In cell series C1 and C2, paste-coated electrodes and UV cured SPEs were used. EC/PC ratios were 2:1 and 1:1 (w/o), respectively, in series C1 and C2. $LiPF_6$ concentration was

1.0 M in the electrolytes. The 1C and 2C discharge capacities at room temperature were more than 90% of those at 0.2C for both C-series cells. When discharged under GSM conditions at −20 °C, cells in series C1 delivered no capacity. Under the same discharge conditions, cells in series C2 delivered an average capacity 7.8% of that at room temperature at low rate.
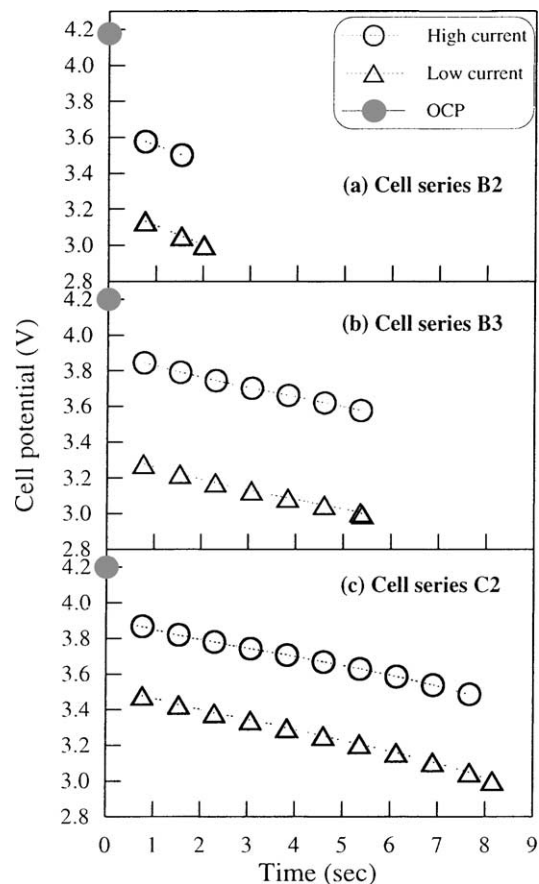

Fig. 3. GSM discharge potential vs. time at −20 °C for cell series B2, B3 and C2, respectively. The triangles and the circles represent potential profiles of high current pulses and low current background, respectively.

Fig. 3(c) shows the GSM discharge potential profile at −20 °C for one of the cells in series C2. The low temperature performance was clearly further improved over cell series B3. The cell in Fig. 3(c) was among those in series C2 whose GSM discharge capacity at −20 °C was about 10% of that at room temperature at low rate.

3.3. Cell impedance at room temperature and at −20°C

Fig. 4 compares typical cell impedance for cell series B and C at room temperature and −20 °C. Here, we use the real component of the interfacial impedance, measured by the total length of the semicircles on the horizontal axis, to compare cell impedance among different groups of cells and between room temperature and −20 °C. For the B series at room temperature, the cell impedance of 2:1 EC/ PC ratio was about three and four times smaller than that of the 1:1 and 1.1:1 EC/PC ratios, respectively; compare Figs. 4(a)–(c). At −20 °C, the cell impedances in series B all increased drastically with respect to that at room temperature. Note that the scales of the horizontal and the vertical axes at −20 °C are 24 times larger than those at
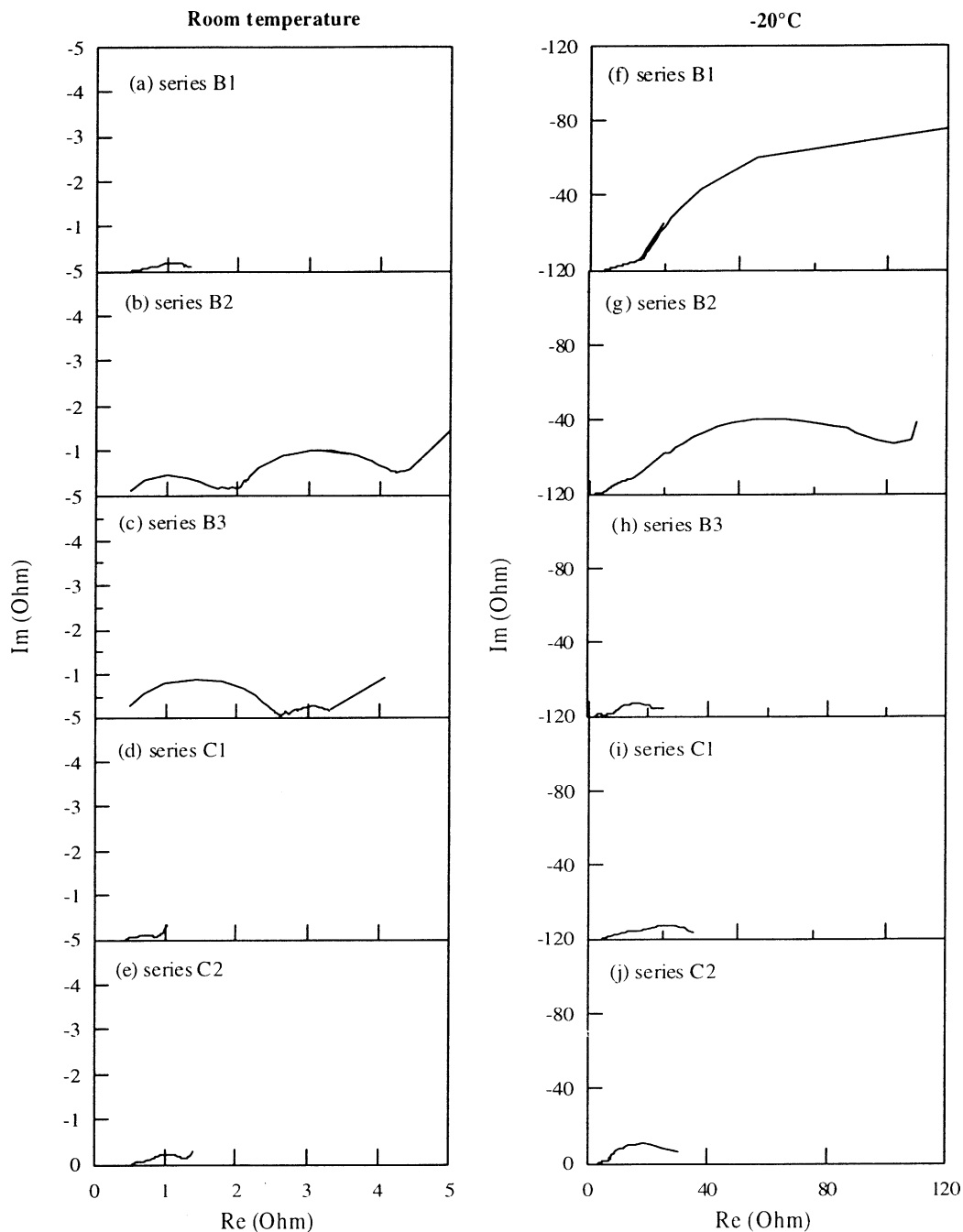

Fig. 4. Electrochemical impedance of cell series B and C at both room temperature and −20 °C.

room temperature, respectively. The cell impedance for series B1, B2 and B3 at −20 °C was about 250, 26, and 8 times, respectively, that at room temperature. Among the B series at −20 °C, B3 had the smallest cell impedance, about 5 and 10 times smaller than that of B2 and B1, respectively. The data showed that the higher the EC content in the solvent, the larger was the increase in cell impedance from room temperature to −20 °C.

The cell impedance data correlated well with the low temperature performance among cells of the B series. The reduced cell capacity at −20 °C under high current pulses was likely due to the dramatic increase in cell impedance.

The impedance data suggested that, at room temperature, the higher EC content in electrolytes benefited cell interfacial properties, as seen by the smaller cell impedance, compared with lower EC content electrolytes. On the other hand, the drastic increase in cell impedance of the higher EC content electrolytes at low temperatures, e.g. −20 °C, was likely due to increased viscosity; compare the freezing point of EC, 36.4 °C, with −49.2 °C of PC.

Figs. 4(d), (e), (i) and (j) compare typical cell impedance spectra for cell series C at both room temperature and −20 °C. The scales in the figure for the C series were kept the same as for the B series, so that direct comparison between series B and C could be made. Note the scales of the horizontal and the vertical axes are different between room temperature and −20 °C. Comparing C1 and C2 series, we have the following observations. (a) At room temperature, the cell impedance in series C1 was about two times smaller than that of C2. This observation is similar to that observed in B series, i.e. higher EC content in electrolytes resulted in smaller cell impedance. (b) At −20 °C, the cell impedance in both C series was increased dramatically, about 69 and 35 times of that at room temperature for EC/PC ratios of 2:1 and 1:1, respectively. The ac impedance of the two C series was comparable at −20 °C; the cell impedance of C2 was about 10% smaller than that of C1.

Comparing B and C series, we have the following observations. (a) For 2:1 and 1:1 EC/PC ratios and at room temperature, the cell impedance in the C series was about two and three times smaller than that in B series, respectively. (b) At −20 °C, the cell impedance in the C series was about seven times smaller than that of B series when EC/PC = 2:1. The values of cell impedance were comparable between B and C series when EC/PC = 1:1.

The above observations showed that cell interfacial properties were influenced by SPE curing methods, especially at low temperature; compare Fig. 4(f) with Fig. 4(i). It is interesting to note that, although the typical cell impedance in C1 at −20 °C was only slightly larger than that of C2, cells in series C1 delivered no GSM discharge capacity at −20 °C, while cells in series C2 delivered an average 7.8% GSM discharge capacity. Since the only difference between C1 and C2 was the EC content, the data suggested
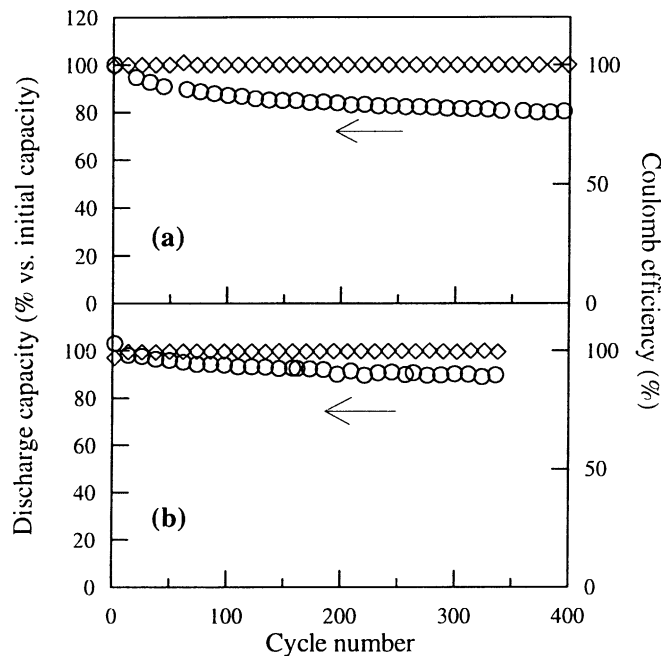

Fig. 5. Capacity retention and Coulomb efficiency vs. cycle number for two of the cells in series C2.

that the low temperature performance was strongly dependent on electrolyte viscosity.

3.4. Long-term cycling

Fig. 5 shows discharge capacity retention versus cycle number for two of the cells in series C2. Coulomb efficiencies versus cycle number are also shown in the figure. The cells were cycled at 0.4C between 2.75 and 4.20 V. The cells had been undergone C rate and low temperature GSM discharge tests before the long-term cycling. The cells in Figs. 5(a) and (b) delivered 97 and 98% of the low rate capacity, respectively, when discharged at 1C rate; and 91 and 96% of the low rate capacity, respectively, when discharged at 2C rate. The cells delivered 8.5 and 7.1% of low rate and room temperature capacities, respectively, under GSM discharge conditions at −20 °C.

The capacity retention versus cycle number curves in Fig. 5 showed similar cycling behavior: an initial quick capacity drop followed by a much slower decline after about 50 cycles. The cell in Fig. 5(a) was cycled 410 times before reaching 80% capacity retention. The cell in Fig. 5(b) maintained 88.7% of the initial capacity after 350 cycles. Fig. 5 shows that both cells were cycled at nearly 100% Coulomb efficiency.

4. Conclusions

For the electrolyte system LiPF$_6$ in EC/PC, the highest ionic conductivity values were found when LiPF$_6$ concen-

tration was around 1.0 M and the EC/PC ratio was around 1:1 (w/o), in the temperature range −20 to 20 °C.

The best low temperature performance of the gelled polymer lithium-ion cells was achieved by using an optimized electrolyte formulation, paste-coated electrodes and UV cured SPEs. Such cells could deliver 10% of the low rate, room temperature capacity under GSM discharge conditions at −20 °C.

The electrochemical impedance study showed that cell impedance with higher EC content in electrolytes was generally much larger than lower EC content electrolytes at low temperatures, e.g. −20 °C. This observation was consistent with the low temperature electrochemical performance, i.e. finite versus nearly zero capacities between low and high EC content electrolytes respectively at −20 °C under GSM discharge conditions. Our study showed that the UV curing method for the SPE provided better interfacial properties than the thermal curing method.

Acknowledgements

References

[1] Y. Ein-Eli, S.F. McDevitt, R. Laura, J. Electrochem. Soc. 145 (1998) L1.
[2] Z.X. Shu et al., J. Electrochem. Soc. 142 (1995) L161.
[3] E.J. Plichta, W.K. Behl, Proceedings of the 38th Power Sources Conference, June 8–11, 1998, Cherry Hill, NJ, USA, p. 444.
[4] M.C. Smart, Abstract 191, in: Proceedings of the 11th International Meeting on Lithium Batteries (IMLB 11), June 23–28, 2002, Monterey, CA, USA.
[5] Ion C. Halalay, Abstract 192, in: Proceedings of the 11th International Meeting on Lithium Batteries (IMLB 11), June 23–28, 2002, Monterey, CA, USA.
[6] F. Coowar, A.M. Christie, P.G. Bruce, C.A. Vincent, J. Power Sources 75 (1998) 144.
[7] M.C. Smart, B.V. Ratnakumar, S. Surampudi, Abstract 333, in: Proceedings of the 196th ECS Meeting, October 17–22, 1999, Honolulu, HI, USA.
[8] T.R. Jow, et al., Abstract 399, in: Proceedings of the 11th International Meeting on Lithium Batteries (IMLB 11), June 23–28, 2002, Monterey, CA, USA.
[9] W. Xing, C. Schlaikjer, Proceedings of the 39th Power Sources Conference, June 12–15, 2000, Cherry Hill, NJ, USA, pp. 294–297.
[10] L. Sun, US Patent 5603982 (1997); US Patent 5609974 (1997).
[11] S. Kuse, T. Kawai, JP2000067866A2 (2000); T. Kawai, JP2000260470-A2 (2000).